On the Fokker-Planck equation for stochastic hybrid systems: application to a wind turbine model

Julien Bect, Yannick Phulpin, Hana Baili, Gilles Fleury

On the Fokker-Planck Equation for Stochastic Hybrid Systems: Application to a Wind Turbine Model

Julien Bect*‡, Yannick Phulpin†‡, Hana Baili*‡, Gilles Fleury*‡
* Dept. of Signal Processing and Electronic Systems
† Dept. of Power and Energy Systems
‡ Supélec, 3 rue Joliot-Curie, Plateau de Moulon, 91192 Gif-sur-Yvette cedex, France.

***Abstract*— This paper presents some recent results concerning a class of continuous-time Markov processes called "stochastic hybrid systems"[1]. These processes describe the evolution of a multidimensional hybrid-state dynamical system subject to Gaussian white noise inputs. After a brief recall of the formalism, we state the generalized Fokker-Planck equation, which is a partial differential equation satisfied by the probability density function of the system. As an illustration, we consider a variable-speed wind turbine, with a switching controller that combines stall regulation and pitch control. For a given value of the mean wind speed, the stationary distribution of the state variables is computed numerically. This truly dynamical analysis of the system yields a complete probabilistic characterization of the uncertain power output, which is much more accurate than the usual static analysis.**

I. Introduction

The dynamical behaviour of a power system typically involves a complex combination of continuous and discrete dynamics [2], the discrete part usually coming from the presence of a switching controller or from an idealized modeling of strong non-linearities. The theory of hybrid dynamical systems [1], [3] is therefore a natural framework for power systems modeling and control, since it allows to simultaneously capture both kinds of behaviour. Although the conventional formulation is deterministic, there have been many attempts to introduce randomness in the theory, in order to cope with the inherent uncertainty in many practical problems (see [4] and the references therein for a survey).

This paper focuses on one class of stochastic hybrid models, called stochastic hybrid systems [5], that we believe potentially useful in the field of power systems. The basic idea is to replace the differential equations in the deterministic model by stochastic differential equations (SDEs) [6]. Roughly, this is tantamount to considering a deterministic hybrid system with Gaussian white noise inputs. An early example of a stochastic hybrid system in the field of power systems can be found in [6]. More generally, such models appear in various application fields [7], [8], [9], notably as the result of stochastic control problems.

[1]In this context, the word "hybrid" indicates a mixture of continuous and discrete state-variables (as in [1], [2] for instance) and has nothing to do with the notion of "hybrid power system".

Our aim is to provide power system practitioners with a short introduction to this modern framework, and especially to a useful mathematical result: the generalized Fokker-Planck Equation (FPE). This is a partial differential equation (PDE) satisfied by the probability density function of the state variables, which provides an alternative to Monte-Carlo techniques for the computation of various probabilistic characteristics of the model.

The paper is organized as follows: in the first part, an abstract definition of stochastic hybrid systems is given and the associated generalized FPE is stated. Then the theory is applied to a variable-speed wind turbine model, yielding a probabilistic characterization of the uncertain power output of the system—for a given mean wind speed. Numerical results are given, that support the usefulness of the approach.

II. Stochastic hybrid processes

A. Definition

A "stochastic hybrid process" is a Markov process $\mathbf{z}(t)$, $t \in \mathbb{R}_+$, that is made up of two components: a discrete component $q(t)$, that takes its values in a countable set $\mathcal{Q}$, and a $\mathbb{R}^n$-valued component $\mathbf{x}(t)$. When the discrete component (sometimes called the mode) is fixed to some value $q_0 \in \mathcal{Q}$, the continuous component evolves in a set denoted by $\overline{\mathcal{X}}_{q_0}$, where $\mathcal{X}_{q_0}$ is an open subset of $\mathbb{R}^n$ and $\overline{\mathcal{X}}_{q_0} = \mathcal{X}_{q_0} \cup \partial\mathcal{X}_{q_0}$ its closure. Therefore, the process $\mathbf{z}(t)$ takes its values in a hybrid state space $\mathcal{Z} \subset \mathcal{Q} \times \mathbb{R}^n$, defined by

$$\mathcal{Z} \;=\; \cup_{q\in\mathcal{Q}} \; \{q\} \times \overline{\mathcal{X}}_q. \tag{1}$$

Various classes of stochastic hybrid processes have been studied in the literature, depending on the kind of jumps and continuous dynamics that are allowed [4]. In this paper, it is assumed that $\mathbf{z}(t)$ satisfies the followings:

- there exists an increasing sequence of Markov times $(\tau_n)_{n\geq 0}$, with $\tau_0 = 0$ and $\tau_n < \tau_{n+1}$ for each n (unless $\tau_n = +\infty$), such that over each interval $[\tau_n; \tau_{n+1})$, $q(t)$ is constant and $\mathbf{x}(t)$ solves a Stratonovich SDE [6]:

$$d\mathbf{x}(t) \;=\; \mathbf{f}(q_n, \mathbf{x}(t))\, dt \;+\; \mathbf{g}(q_n, \mathbf{x}(t))\, dB(t), \tag{2}$$

  where $q_n = q(\tau_n)$ and $B(t)$ is a standard Brownian motion;

- there exists a subset G of the boundary $\partial\mathcal{Z} = \cup_{q\in\mathcal{Q}} \{q\}\times\partial\mathcal{X}_q$, called the guard set, such that the jump times τ_n satisfy the recursive relation:

$$\tau_n \;=\; \inf\left\{\, t > \tau_{n-1} \,|\, \mathbf{z}(t^-) \in G \,\right\}, \tag{3}$$

  for all $n \geq 1$, i.e. τ_n is the time where the process $\mathbf{z}(t)$ first reaches the guard set after τ_{n-1};
- there exists a function $\Phi : G \to \mathcal{Z} \setminus G$, called the reset map, such that the state of the process after a jump at time τ_n, $n \geq 1$, is given by $\mathbf{z}(\tau_n) = \Phi(\mathbf{z}(\tau_n^-))$.

The reader is referred to [6] for the basic definitions concerning Markov processes and SDEs. The class of processes under consideration is very close to the stochastic hybrid systems of [5], with some minor modifications.

Formally, the SDE (2) can also be written as

$$\dot{\mathbf{x}}(t) \;=\; \mathbf{f}(q_n, \mathbf{x}(t)) \;+\; \mathbf{g}(q_n, \mathbf{x}(t))\, w(t), \tag{4}$$

where $w(t) = \dot{B}(t)$ is a Gaussian white noise. The whiteness assumption is not as restrictive as it seems. Indeed, colored noises can be considered as well in this framework, using a shaping filter with $w(t)$ as an input. An example of this is provided in section III-B.

B. The generalized Fokker-Planck equation

The state $\mathbf{z}(t)$ of the process at time $t \geq 0$ is a hybrid random variable, which is fully characterized by the joint probability law of $\mathbf{x}(t)$ and $q(t)$. In this section, it is assumed that a pdf $\wp(q_0, x_0, t)$ exists, such that

$$\mathbb{P}\left\{\, q(t) = q_0,\, \mathbf{x}(t) \in B \,\right\} \;=\; \int_B \wp(q_0, \mathbf{x}_0, t)\, d\mathbf{x}_0\,, \tag{5}$$

for any measurable $B \subset \mathbb{R}^n$.

The dynamics of $t \mapsto \wp(q_0, x_0, t)$ is given by the generalized Fokker-Planck equation, which will be stated below. The equation extends the usual FPE [10, chap. 5], [6, pp 168–169], which applies to diffusion processes defined by SDEs like (2), to the class of stochastic hybrid processes defined in II-A.

a) Generalized FPE, local part: the first part of the result is that, on $\mathcal{Z} \setminus (G \cup \Phi(G))$, the pdf satisfies the usual FPE:

$$\frac{\partial\wp}{\partial t} + \mathrm{div}(\mathbf{j}) \;=\; 0\,, \tag{6}$$

where div denotes the divergence operator with respect to the continuous variables of the state space, and $\mathbf{j}$ is the so-called probability current, defined componentwise by:

$$\mathbf{j}_t^k \;=\; \mathbf{f}^k\, \wp_t \;-\; \frac{1}{2}\, \mathbf{g}^k\; \mathrm{div}(\wp_t\, \mathbf{g})\,. \tag{7}$$

Equation (6) is a local conservation equation, which accounts for the fact that, between its jumps, the process evolves continuously according to the SDE (2). Note that this single equation actually hides a system of PDEs—one for each mode.

b) Generalized FPE, non-local part: the jumping behaviour of the process $\mathbf{z}(t)$ translates to the pdf level as a discontinuity in the probability current $\mathbf{j}(t)$ on $H = \Phi(G)$. To express this, the outward and inward probability currents are defined—respectively on G and H—by:

$$\mathbf{j}_t^{\text{out}} \;=\; \mathbf{j}_t \,.\, \mathbf{n}\,, \tag{8}$$

$$\mathbf{j}_t^{\text{in}} \;=\; (\mathbf{j}_t^{(2)} - \mathbf{j}_t^{(1)}) \,.\, \mathbf{n}_{12}\,, \tag{9}$$

where $\mathbf{n}$ is the outward-pointing unit normal on G, and $\mathbf{n}_{12}$ the unit normal on H directed from side 1 to side 2. Then, assuming that Φ is a bijection between G and H, the following relation holds:

$$\mathbf{j}^{\text{out}}(\mathbf{z}_0, t) \;=\; |\Phi'|\; \mathbf{j}^{\text{in}}(\Phi(\mathbf{z}_0), t)\,, \tag{10}$$

for all $\mathbf{z}_0 \in G$, with $|\Phi'|$ the Jacobian determinant of Φ. This equation has a nice physical interpretation: the probability current $\mathbf{j}^{\text{out}}$ flows out of the state space through the "sink" G, and is instantaneously reinjected by the "source" H.

c) Generalized FPE, boundary conditions: let G^* and H^* be the subsets of G and H where the vector field $\mathbf{g}$ is not tangential. Then the pdf $\wp_t$ is continuous on H^* and vanishes on G^*.

A proof of the generalized FPE can be found in [11] for the one-dimensional case, and more recently [12] for the multi-dimensional case. Both rely on the a priori assumption that a smooth enough pdf exists—a very reasonable assumption in most practical applications.

III. Application

As an application, the generalized Fokker-Planck equation will now be used to assess the uncertainty in the power output of a variable-speed wind turbine. The system is modeled as a hybrid dynamical system whose input and output are respectively the wind speed $v(t)$ and the generator power output $P_{\text{G}}(t)$. The model is presented in sections III-A and III-B. Then the Fokker-Planck equation is stated in III-C, and the stationarity assumption is discussed in section III-D. Finally, numerical results are obtained and compared to brute-force Monte-Carlo simulations in section III-E.

A. Modeling the wind turbine and its hybrid controller

The dynamics of the wind turbine is given by the angular momentum theorem:

$$J\,\frac{d\omega}{dt} \;=\; \frac{P_{\text{drive}} - P_{\text{brake}}}{\omega} \tag{11}$$

where ω is the rotor speed, J the moment of inertia, P_{drive} the aerodynamic power captured by the wind turbine and P_{brake} the braking power from the generator. The generator power output is related to the braking power by the simple relation $P_{\text{G}} = \eta\, P_{\text{brake}}$, where η is assumed constant. The aerodynamic power is given by the algebraic relation

$$P_{\text{drive}} \;=\; \frac{\pi}{2}\,\rho\, R^2\, c_{\text{p}}(\lambda, \theta)\, v^3, \tag{12}$$

where ρ is the air density, R the rotor radius, θ the pitch angle, $\lambda = R\omega/v$ the tip speed ratio (TSR) and c_{p} the power

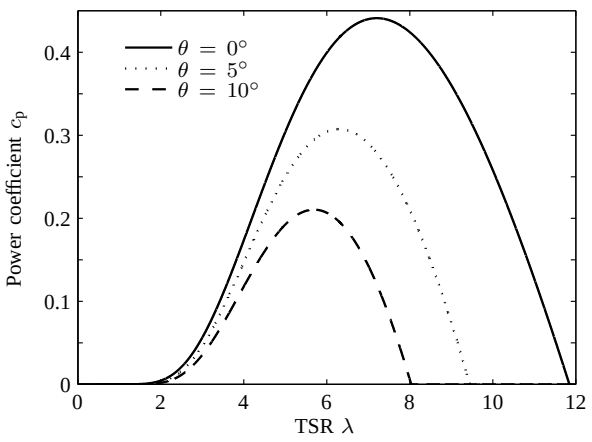

Fig. 1. Power coefficient versus TSR

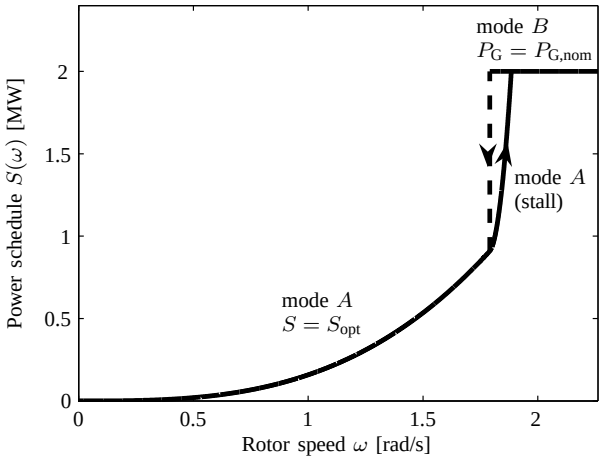

Fig. 2. Power schedule $\omega \mapsto S(\omega)$

coefficient. A numerical approximation of c_p is provided in [13]. Fig. 1 depicts the $\lambda \mapsto c_p(\lambda, \theta)$ characteristic, for several values of the pitch angle θ. We denote by $c_{p,opt}$ the maximum of $c_p(\lambda, 0)$, which is attained for a unique optimal TSR λ_{opt}.

The turbine is operated by a switched controller inspired from [14], with two discrete modes. In mode A (lower to medium wind speed region), the rotor speed is controlled by adjusting the generator power output P_G, following a given power schedule $P_G = S(\omega)$ that is explained below. It is assumed that the generator can respond to the power command almost instantaneously. In mode B (higher wind speed region), the output power is kept constant to its nominal value $P_{G,nom}$, and the aerodynamic power P_{drive} is adjusted using pitch control, in order to maintain ω around its nominal value ω_{nom}. The controller switches from mode A to mode B when $\omega = \omega_{nom}$, and back to mode A when $\omega = \omega_{BA} < \omega_{nom}$. The strict inequality defines a hysteretic behaviour, which is necessary in order to prevent chattering between A and B.

In mode A, the turbine is operated to stay as close as possible to the optimal TSR λ_{opt}. To achieve that, the power schedule is set to

$$S(\omega) \;=\; S_{opt}(\omega) \;=\; \frac{\pi}{2}\,\eta\,\rho\,R^2\,c_{p,opt}\left(\frac{R\omega}{\lambda_{opt}}\right)^3. \qquad (13)$$

This ensures that, for fixed θ and v, the rotor speed $\omega = \lambda_{opt} v/R$ is a stable equilibrium (in fact, there are only two stable equilibrium points, the other one being $\omega = 0$). For a smooth transition between modes A and B, the output power is raised progressively to $P_{G,nom}$ between ω_{BA} and ω_{nom}, thereby driving the turbine into the aerodynamic stall region. The resulting power schedule is shown on Fig. 2.

In mode B, following [13], a proportional controller is used for the pitch angle:

$$\frac{d\theta}{dt} \;=\; \begin{cases} 0 & \text{if } \theta = 0 \text{ and } \omega \le \omega_{nom}, \\ 0 & \text{if } \theta = \theta_{max} \text{ and } \omega \ge \omega_{nom}, \\ h\left(K\left(\omega - \omega_{nom}\right)\right) & \text{otherwise,} \end{cases} \qquad (14)$$

where h is the limiter function

$$h(\dot\theta) = \min\left(\dot\theta_{max}, \max\left(\dot\theta_{min}, \dot\theta\right)\right).$$

B. Modeling the wind speed

Realistic wide band models of the horizontal wind speed $v(t)$ have to account for a wide range of time scales, ranging from high frequency turbulent phenomena to daily and monthly fluctuations [15]. Consequently, our analysis will be carried over short time intervals of about an hour, where $v(t)$ can be modeled [16] as a stationary Gaussian process with hourly mean $\bar v$ and standard deviation $\sigma = \kappa \bar v$. The factor κ depends on the geographical location of the wind turbine site.

Several power spectral densities (PSD) have been proposed in the literature for the short-term turbulent component of the wind speed, among which Von Karman's spectrum [15], [17] and Kaimal's spectrum [13], [17]. Both decay like $f^{-5/3}$ at infinity, a feature that cannot be reproduced by Brownian-driven stochastic differential equations[2]. Therefore, we use a simple one-dimensional SDE [18] to decribe $v(t)$:

$$dv(t) \;=\; -\,\frac{v(t) - \bar v}{T}\,dt \;+\; \kappa\,\bar v\,\sqrt{2/T}\,dB(t) \qquad (15)$$

where $T = L/\bar v$, with L the turbulence length scale. Higher order SDEs, such as the one proposed in [15], could be used to obtain a better approximation of the forementioned PSDs. However, this does not seem necessary in the problem under consideration, since the highest frequency fluctuations are very local and therefore even out over the rotor surface [13]. Furthermore, it would increase the number of continuous variables, making the numerical solution of the PDE much more difficult if not impossible.

The SDE (15) defines a stochastic process that can take negative values. A reflecting boundary is added at $v = 0$ to ensure that the process stays positive at all times.

[2]SDE driven by fractional Brownian motions can produced this kind of PSDs but are outside the scope of our method.

C. The generalized Fokker-Planck equation

Except for the presence of the reflecting barrier at $v = 0$, the stochastic model just defined belongs to the class of stochastic hybrid systems described in II-A:

- the continuous component is the vector-valued process $\mathbf{x}(t) = (\omega(t), \theta(t), v(t))$, whose dynamics is given by equations (11), (14) and (15);
- the discrete component is the state $q(t) \in \{A, B\}$ of the switching controller;
- and the reset map Φ toggles the discrete component between modes A and B without affecting the continuous components, i.e. $\Phi(\mathbf{x}_0, A) = (\mathbf{x}_0, B)$ and vice versa (the corresponding state space is depicted on Fig. 3).

The generalized FPE of section II-B will now be made explicit for this model. The probability current (7) simplifies to

$$\left\{ \begin{array}{rcl} \mathbf{j}_t^\omega & = & \mathbf{f}^\omega \, \wp_t \\ \mathbf{j}_t^\theta & = & \mathbf{f}^\theta \, \wp_t \\ \mathbf{j}_t^v & = & \mathbf{f}^v \, \wp_t \, - \, D \, \frac{\partial \wp_t}{\partial v} \end{array} \right.$$

where $D = \kappa^2 \bar{v}^2 / T$ and $\mathbf{f}$ is the deterministic part in the right-hand sides of (11), (14) and (15). Therefore, according to II-B.a, the usual FPE

$$\frac{\partial \wp}{\partial t} \; = \; D \, \frac{\partial^2 \wp}{\partial v^2} \, - \, \mathrm{div}(\mathbf{f} \wp)$$

holds on the four components of the state space, denoted by $\mathcal{X}_A^1$, $\mathcal{X}_A^2$, $\mathcal{X}_B^1$ and $\mathcal{X}_B^2$ on Fig. 3. Furthermore, by II-B.b, the pdf has a discontinuity on the set $H = \Phi(G)$. Indeed, for $\mathbf{z}_0 = (\mathbf{x}_0, B) \in G$, equation (10) becomes

$$- \, \mathbf{f}^\omega(\mathbf{z}_0) \, \wp(\mathbf{z}_0, t) \; = \; \mathbf{f}^\omega(\mathbf{z}_1) \, \left[\wp(\mathbf{z}_1^+, t) - \wp(\mathbf{z}_1^-, t) \right] \, ,$$

where $\mathbf{z}_1^\pm = (\omega_0^\pm, \theta_0, v_0, A)$. A similar equation holds for the other part of the guard—i.e. for $\mathbf{z}_0 = (\mathbf{x}_0, A) \in G$. The boundary conditions II-B.c do not apply here, since the sets G^* and H^* are empty (the vector field $\mathbf{g}$ is parallel to the v-axis and therefore is tangential to G and H). Finally, the reflecting barrier for the wind speed v translates as a no-flux boundary condition $\mathbf{j}_t^v = 0$ on the surface $\{v = 0\}$.

Remark: a careful study of the dynamics actually reveals that the probability law of $\mathbf{x}_t$ is "degenerate" in this model, because there can be a non-zero probability that $\theta_t = 0$ or $\theta_t = \theta_{\max}$. Therefore, the first assumption of section II-B—that a pdf exists—is not totally fulfilled. However, slight modifications of the theory (omitted here for the sake of conciseness) allow to write a generalized FPE anyway.

D. Stationary regime

The generalized FPE can be used to study the stochastic system either in transient regime—i.e. on a time interval $[0; T]$, for a given initial distribution $\wp_0$—or in stationary regime. In the problem under consideration, which is the assessment of the power output uncertainty as a function of the mean wind speed $\bar{v}$, the latter approach seems more appropriate since no relevant initial distribution can be specified. In practice, this will lead to the computation of a time-independent distribution

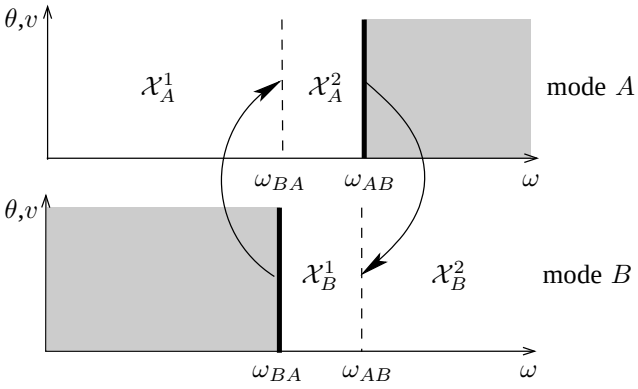

Fig. 3. State space for the wind turbine model. The curved arrows indicate the action of the reset map Φ. The bold and dashed lines symbolize respectively the guard G and the set $H = \Phi(G)$.

$\wp(\mathbf{z}|\bar{v})$, which is the stationary distribution for a fixed $\bar{v}$. This method is justified by the fact that $\bar{v}(t)$ is a "slow" variable with respect to the "fast" variable $\mathbf{z}(t)$: as a response to a small change $\bar{v}_0 \to \bar{v}_0'$ of the mean wind speed, the distribution of $\mathbf{z}(t)$ conditionally to $\bar{v}(t)$ relaxes quickly from $\wp(\mathbf{z}|\bar{v}_0)$ to $\wp(\mathbf{z}|\bar{v}_0')$, and therefore can be approximated by $\wp(\mathbf{z}|\bar{v}(t))$ at all times.

Unfortunately, the only exact stationary distribution in this model corresponds to the wind turbine being almost surely stopped ($\omega(t) = 0$). Indeed, extreme wind gusts of arbitrarily large magnitude and duration are theoretically possible in the wind model (15). In mode A, this can take the system into the unstable region [18] and consequently force the turbine to stop. However, such an event is extremely rare and is in fact just a consequence of the simplified modeling of the system. The "interesting" behaviour of the system—when the wind turbine is working properly—is only a quasi-stationary solution, i.e. a probability distribution that is almost invariant and relaxes very slowly to the exact stationary solution[3]. Numerically, a well-chosen truncation of the computational domain allows to find the quasi-stationary solution, which is of practical interest, instead of the undesirable exact one.

E. Numerical results

The numerical results presented in this section are computed for a 2 MW variable speed wind turbine, the characteristics of which are given in [13]. The thresholds for the switching controller are set to $\omega_{\mathrm{AB}} = \omega_{\mathrm{nom}} = 18\,\mathrm{RPM}$ and $\omega_{\mathrm{BA}} = 0.95\,\omega_{\mathrm{AB}}$ (see Fig. 2). The PDE is discretized in space using a finite volume scheme [20]. The stationary distribution is computed directly using Arnoldi's method[4], as the positive and normalized eigenvector corresponding to the eigenvalue

[3]This can be made more rigourous using the concepts of metastable sets and exit rates, see [19] for instance.

[4]This algorithm allows to compute a few eigenvalues of a large sparse matrix. It is implemented in ARPACK [21] and available in Matlab's `eigs` function.

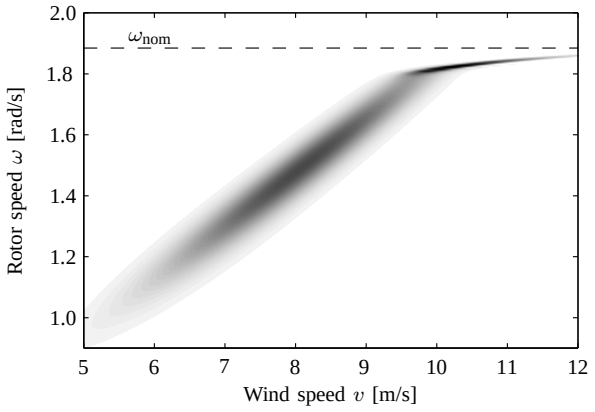

(a) $\bar{v} = 8\,m/s$

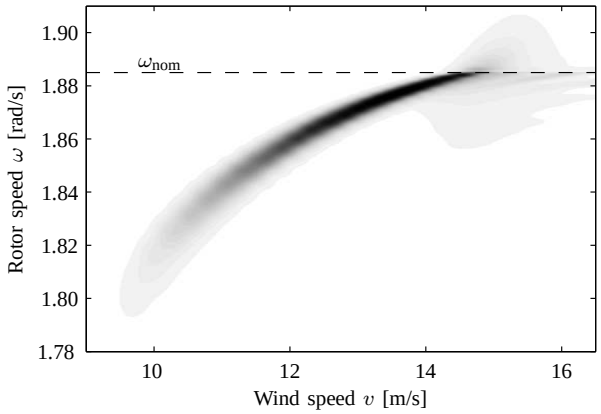

(b) $\bar{v} = 13\,m/s$

Fig. 4. Joint pdf of the rotor speed $\omega(t)$ and the wind speed $v(t)$, obtained by marginalization over the pitch angle $\theta(t)$ and the mode $q(t)$.

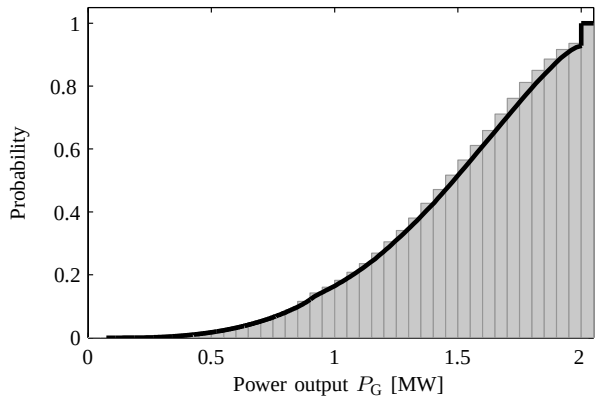

Fig. 5. Distribution function of the power output P_{G}, for a mean wind speed $\bar{v} = 12m/s$: result obtained with the generalized FPE (full line), compared to a reference Monte-Carlo simulation (cumulative histogram).

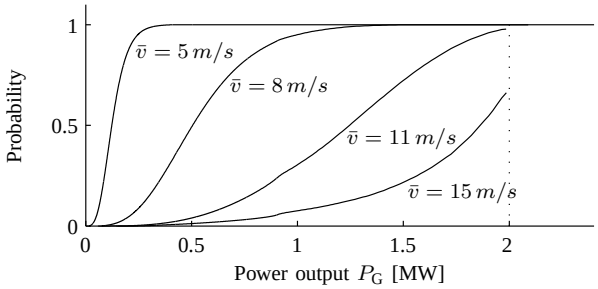

Fig. 6. Distribution function of the power output P_{G}, for several values of the mean wind speed $\bar{v}$. The discontinuity at $P_{\text{G}} = P_{\text{G,nom}}$ for high wind speeds indicates that $\mathbb{P}\{q(t) = B\} > 0$.

zero. This approach is very efficient since—contrary to MC-based methods—no time-marching is required. The resulting joint pdf of the rotor speed $\omega(t)$ and the wind speed $v(t)$, obtained by marginalization over the pitch angle $\theta(t)$ and the mode $q(t)$, is shown on Fig. 4 for two differerent values of the mean wind speed $\bar{v}$. Other marginal pdf's could be obtained as well.

The generator power output $P^G(t)$ is a function of the rotor speed $\omega(t)$ and the discrete mode $q(t)$. Therefore, its probability law can be deduced from the joint pdf of the state variables. Since the random variable $P^G(t)$ has a mixed probability measure, involving an absolutely continuous component coming from mode A, and a discrete component from mode B, it is more convenient to consider its distribution function: $F(P_{\text{G},0}) = \mathbb{P}\{P_{\text{G}}(t) \leq P_{\text{G},0}\}$. Fig. 5 shows a good agreement between the result obtained by the Fokker-Planck equation and a reference cumulative histogram obtained by Monte-Carlo simulation of the system (using the Euler scheme with approximately 5.10^6 time steps of duration $\delta t = 0.01\,s$). Then, solving the PDE repeatedly with varying $\bar{v}$, it becomes possible to characterize the uncertainty in the power output as a function of the mean wind speed (see Fig. 6 and 7). This a truly dynamical result, much more accurate than the usual static analysis: indeed, both the fluctuations of the wind speed and the switchings of the controller are taken into account here, whereas the static analysis assumes the steady-state relationship between $\bar{v}$ and P_{G}.

Computationally speaking, the PDE-based method seems faster than MC-based methods for this problem. The main reason is that, as mentionned earlier, the stationary distribution can be computed directly with the PDE approach, whereas MC techniques require the simulation of the system until the stationary regime takes place. Using Matlab on a Pentium IV (2.8 GHz, 1 Go of memory), the pdf's of Fig. 4 are obtained in approximately 1 minute; comparatively, a basic MC method takes about 10 minutes to produce a "stable" approximation of the distribution function shown on Fig. 5. A more precise comparison is out of the scope of this paper, since both approaches involve the tuning of many parameters (moreover, the convergence of a MC-based method can be improved by variance reduction techniques).

More generally, the use of PDE-based methods is restricted

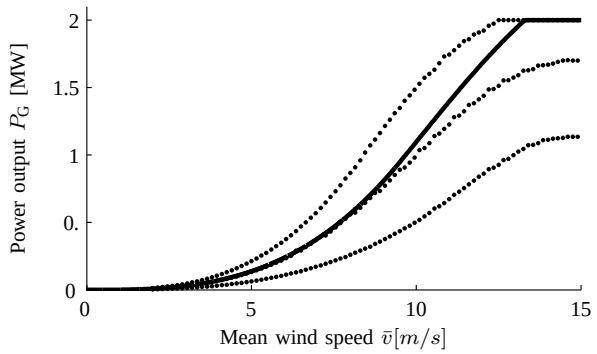

Fig. 7. Power output P_G as a function of the mean wind speed: static (full line) and probabilistic (dotted lines) analysis. From bottom to top, the dotted lines show the 10th percentile, the mean and the 90th percentile.

to models of low dimension—approximately $n \leq 4$ at the present time—by memory requirements and complexity issues. When $n \leq 3$, they can be more efficient that MC-based methods, especially when the stationary regime is to be computed. On the opposite, when $n \geq 5$, the numerical solution of the PDE becomes unfeasible.

IV. Conclusion

The generalized Fokker-Planck equation for stochastic hybrid systems has been presented and applied to a variable-speed wind turbine model. From a methodological point of view, this shows that PDE-based methods can profitably replace Monte-Carlo simulation for the dynamical analysis of stochastic hybrid models—at least when the number of continuous variables and discrete states allows the numerical solutions of the PDE. Concerning the wind turbine application, the distribution function of the generator power output has been computed, for a wide range of mean wind speeds. A similar approach could be used with virtually any kind of wind turbine and control strategy, therefore providing power systems operators with an efficient numerical tool to assess a priori the uncertainty in the power output of a wind power plant. On a larger scale, this approach could hopefully provide some assistance for the network integration of wind parks.

References

[1] A. J. van der Schaft and H. Schumacher, *An Introduction to Hybrid Dynamical Systems*, ser. LNCIS. Springer-Verlag, 2000, vol. 251.

[2] I. A. Hiskens and M. A. Pai, "Hybrid systems view of power system modelling," in *IEEE International Symposium on Circuits and Systems, ISCAS 2000*, Geneva, Switzerland, May 2000.

[3] G. Labinaz, M. M. Bayoumi, and K. Rudie, "A survey of modeling and control of hybrid systems," *Annual Reviews in Control*, vol. 21, pp. 79–92, 1997.

[4] G. Pola, M. Bujorianu, J. Lygeros, and M. D. Benedetto, "Stochastic hybrid models: an overview," in *IFAC Conference on the Analysis and Design of Hybrid Systems*, June 2003.

[5] J. Hu, J.Lygeros, and S. Sastry, "Towards a theory of stochastic hybrid systems," in *Hybrid Systems: Computation and Control, Third International Workshop, HSCC 2000*, ser. LNCS, N. Lynch and B. H. Krogh, Eds. Springer-Verlag, 2000, pp. 160–173.

[6] B. Øksendal, *Stochastic Differential Equations*. Springer-Verlag, 1985.

[7] L. H. R. Alvarez, "Stochastic forest stand value and optimal timber harvesting," *SIAM Journal on Control and Optimization*, vol. 42, pp. 1972–1993, 2004.

[8] A. Dixit, "Entry and exit decisions under uncertainty," *Journal of Political Economy*, vol. 97, pp. 620–638, 1989.

[9] Y. Xu and J. Hespanha, "Communication logics for networked control systems," in *Proceedings of the 2004 American Control Conference*, June 2004, pp. 572–577.

[10] C. Gardiner, *Handbook of Stochastic Methods for Physics, Chemistry and the Natural Sciences*. Berlin: Springer-Verlag, 1985.

[11] R. Malhamé and C.-Y. Chong, "Electric load model synthesis by diffusion approximation of a high-order hybrid-state stochastic system," *IEEE Trans. Automat. Contr.*, vol. 30, no. 9, pp. 854–860, September 1985.

[12] J. Bect, H. Baili, and G. Fleury, "Generalized Fokker-Planck equation for piecewise-diffusion processes with boundary hitting resets," 2005, submitted to the 17th International Symposium on the Mathematical Theory of Networks and Systems (MTNS 2006).

[13] J. G. Slootweg, H. Polinder, and W. L. Kling, "Representing wind turbine electrical generating systems in fundamental frequency simulations," *IEEE Transactions on Energy Conversion*, vol. 18, no. 4, pp. 516–524, December 2003.

[14] E. Muljadi and C. P. Butterfield, "Pitch-controlled variable-speed wind turbine generation," *IEEE Transactions on Industry Applications*, vol. 37, pp. 240–246, 2001.

[15] C. Nichita, D. Luca, B. Dakyo, and E. Ceanga, "Large band simulation of the wind speed for real time wind turbine simulators," *IEEE Transactions on Energy Conversion*, vol. 17, no. 4, pp. 523–529, December 2002.

[16] E. Welfonder, R. Neifer, and M. Spanner, "Development and experimental identification of dynamic models for wind turbines," *Control Engineering Pratice*, vol. 5, no. 1, pp. 63–73, 1997.

[17] P. S. Veers, "Three-dimensional wind simulation," Sandia National Laboratories, Albuquerque, Tech. Rep. SAND88-0152, March 1988.

[18] T. Ekelund, "Speed control of wind turbines in the stall region," in *Proceedings of the Third IEEE Conference on Control Applications*, Glasgow, UK, 1994, pp. 227–232.

[19] C. Schütte, W. Huisinga, and S. P. Meyn, "Metastability of diffusion processes," in *Proceeding of the IUTAM Symposium on Nonlinear Stochastic Dynamics*, 2003.

[20] R. Eymard, T. Gallouët, and R. Herbin, *Handbook of Numerical Analysis, Vol. VII*. North-Holland / Elsevier, 2000, ch. Finite volume methods, pp. 713–1020.

[21] R. B. Lehoucq, D. C. Sorensen, and C. Yang, *ARPACK User's Guide – Solution of Large-scale Eigenvalue Problems with Implicitly Restarted Arnoldi Methods*, ser. SIAM series in software, environments and tools. SIAM, 1998, no. ISBN 0-89871-407-9.